Real-Time Selective Harmonic Minimization for Multilevel Inverters Connected to Solar Panels Using Artificial Neural Network Angle Generation

Faete Filho, *Student Member, IEEE*, Leon M. Tolbert, *Senior Member, IEEE*, Yue Cao, *Student Member, IEEE*, and Burak Ozpineci, *Senior Member, IEEE*

***Abstract*—This work approximates the selective harmonic elimination problem using artificial neural networks (ANNs) to generate the switching angles in an 11-level full-bridge cascade inverter powered by five varying dc input sources. Each of the five full bridges of the cascade inverter was connected to a separate 195-W solar panel. The angles were chosen such that the fundamental was kept constant and the low-order harmonics were minimized or eliminated. A nondeterministic method is used to solve the system for the angles and to obtain the data set for the ANN training. The method also provides a set of acceptable solutions in the space where solutions do not exist by analytical methods. The trained ANN is a suitable tool that brings a small generalization effect on the angles' precision and is able to perform in real time (50-/60-Hz time window).**

***Index Terms*—Artificial neural network, cascade, genetic algorithm, harmonic elimination, multilevel inverter, photovoltaic.**

I. Introduction

A NUMBER OF technical papers using selective harmonic elimination (SHE) or minimization have been reported for fundamental frequency operation using the most common multilevel (ML) inverter topologies [1]–[3]. The cascade ML configuration has independent dc sources that may have different voltage levels. Those dc sources might be capacitors, fuel cells, or solar panels and will consequently bring a voltage imbalance depending on the system dynamics. Numerous papers have been reported using SHE or selective harmonic minimization of cascaded ML inverters.

In [4], genetic algorithms (GAs) have been used to determine the optimal switching angles for dc sources of equal values. Analytical solutions for this problem using the theory of symmetric polynomials were also reported for unipolar and bipolar schemes [5], [6]. All of these papers assumed that the dc sources are equal and do not vary with time. In [7] and [8], analytical solutions for the case of unequal dc sources have been derived, and in [9]–[12], algorithms to solve for the angles have been proposed. Also, in [13] and [14], a more general approach is formulated for the m-level n-harmonic case. All of these papers use computationally intensive time-consuming equations to solve for the angles; therefore, the switching angles are calculated offline.

The authors in [15] and [16] have developed methods to calculate the switching angles in real time; however, their approach was not extended for unequal dc sources. An alternate approach to determine the optimum switching angles in real time for varying dc sources is to calculate the switching angle solutions offline and store the solutions in a lookup table. For accurate representation of every solution for every different dc source case, a large lookup table would be required. Even then, for some operating points, the solutions might be missing, and some type of interpolation would be required. In terms of lookup table size requirements, a 32-b floating-point DSP would require at least 40 B per row with ten floating numbers per row. That means 25 rows of data for each 1 kB not including memory space for program code.

In this paper, the lookup table is replaced by an artificial neural network (ANN), which, if well trained, has the inherent capability of generalizing solutions [17]. What this means is that, if the correct range of data is used for training and if the ANN is not overtrained, the network will fill in the solution gaps properly. Since ANN runs fast, it is possible to quickly determine the switching angles to establish real-time control.

II. Approach to the Problem and Methodology

A system's overview of the 11-level cascade H-bridge (CHB) inverter and control is shown in Fig. 1. It has a five-full-bridge series-connected configuration with five solar panels as its

Manuscript received November 15, 2010; revised February 9, 2011; accepted March 14, 2011. Date of publication July 18, 2011; date of current version September 21, 2011. Paper 2010-IPCC-498.R1, presented at the 2010 IEEE Energy Conversion Congress and Exposition, Atlanta, GA, September 12–16, and approved for publication in the IEEE Transactions on Industry Applications by the Industrial Power Converter Committee of the IEEE Industry Applications Society.

F. Filho is with the Department of Electrical Engineering and Computer Science, The University of Tennessee, Knoxville, TN 37996-2100 USA (e-mail: ffilho@utk.edu).

L. M. Tolbert is with the Department of Electrical Engineering and Computer Science, The University of Tennessee, Knoxville, TN 37996-2100 USA, and also with the Power Electronics and Electric Machinery Research Center, Oak Ridge National Laboratory, Knoxville, TN 37932 USA (e-mail: tolbert@utk.edu).

Y. Cao was with the Department of Electrical Engineering and Computer Science, The University of Tennessee, Knoxville, TN 37996-2100 USA. He is now with the University of Illinois at Urbana–Champaign, Champaign, IL 61820 USA (e-mail: ycao6@utk.edu).

B. Ozpineci is with the Power Electronics and Electric Machinery Group, Oak Ridge National Laboratory, Oak Ridge, TN 37831 USA (e-mail: burak@ornl.gov).

Color versions of one or more of the figures in this paper are available online at http://ieeexplore.ieee.org.

Digital Object Identifier 10.1109/TIA.2011.2161533

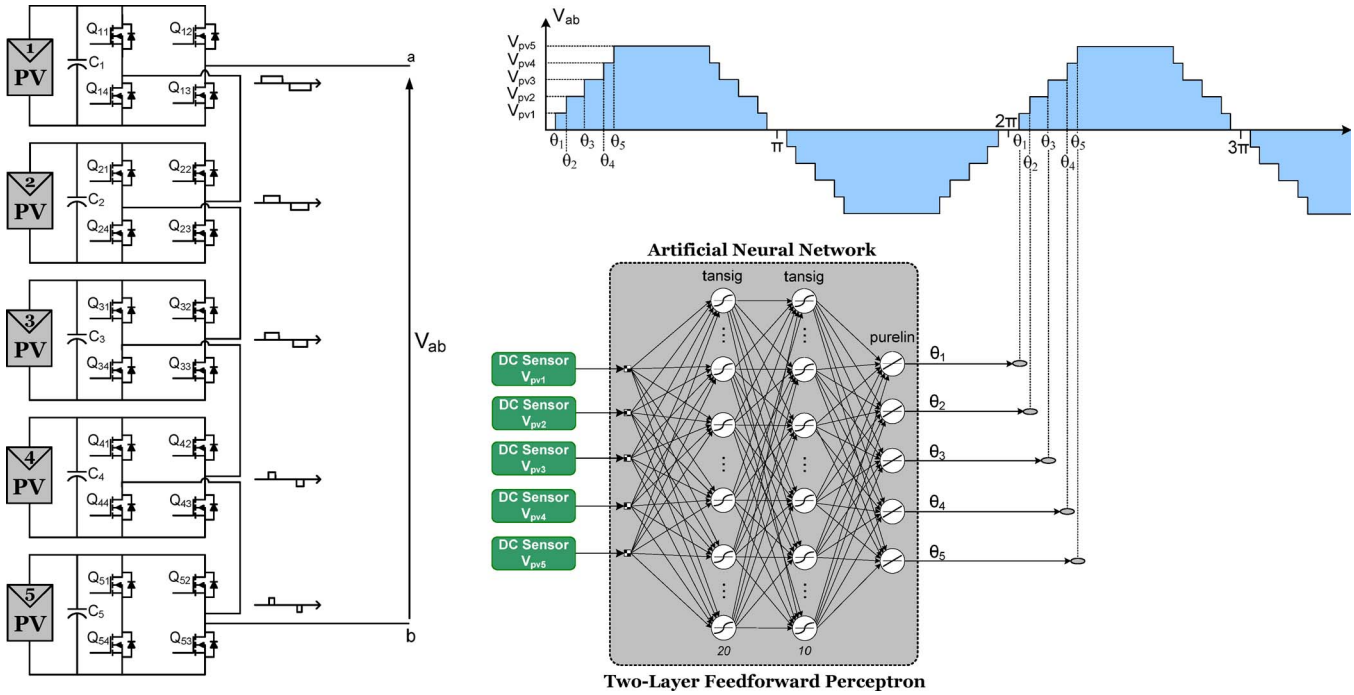

Fig. 1. Single-phase ML cascade inverter topology and ANN-based angle control.

isolated input dc supply that may have different voltage levels and/or dynamics if the photovoltaic (PV) modules connected to each H-bridge have different solar irradiation.

A. SHE and Unequal DC Sources

Equation (1) shows the contents of the output voltage at infinite frequencies. The module voltages V_{PV1}–V_{PV5} are associated to their respective switching angles θ_1–θ_5. This equation includes only odd nontriplen harmonics. The reason for that lies on the assumptions of wave symmetry that cancels out the even components, and also in a three-phase application, the multiples of the third harmonic vectors will add up to zero in the line voltage of a three-phase balanced system. The target harmonics can be arbitrarily set, a new data set can be found, and a new ANN can be trained for the system. The selection of target harmonics is dependent upon the application requirements. Equation (1) is the core equation and also the starting point for SHE. The target harmonics in (1) will define the set of transcendental equations to be solved. It is desired to solve (1) so that, under variations in the dc input sources, the fundamental output voltage is maintained and the lowest nontriplen harmonics (in this case, the 5th, 7th, 11th, and 13th) are canceled

$$V_{ab}(wt) = \sum_{n=1,5,7,11,13,\ldots}^{\infty} \times \left[\frac{4}{\pi \cdot n} \cdot (V_{\mathrm{PV1}} \cos(n \cdot \theta_1) + V_{\mathrm{PV2}} \cos(n \cdot \theta_2) + V_{\mathrm{PV3}} \cos(n \cdot \theta_3) + V_{\mathrm{PV4}} \cos(n \cdot \theta_4) + V_{\mathrm{PV5}} \cos(n \cdot \theta_5)) \right]. \quad (1)$$

Many dc sources such as solar panels and fuel cells have varying output voltages depending on varying sunlight intensity, load, or other factors. For grid connection, either a dc–dc converter is used to regulate this dc voltage or the modulation index of the grid-interface inverter is varied depending on the dc voltage level. For example, during a day of operation, the solar panel output voltage may vary according to the amount of energy available, and the grid-interface system should be able to respond to this variation in the switching angles to keep the fundamental regulated at its reference value and the low-order harmonics minimized.

The approach in this work is to maintain the fundamental at the desired level by means of choosing the low-frequency switching angles in (1) as shown in Fig. 1. Instead of using an analytic method to determine the angles offline, this paper uses a nondeterministic approach to solve for the angles. This methodology can give some insight about the convergence of the solution in the space where no solution can be found by the analytical approach. In this manner, a GA was implemented to find the switching angles (offline) for a set of predetermined input voltages of an 11-level cascade inverter. A sample of this data set is presented in Table I. An important feature of the GA for this approach is that, for the range space where there is no analytical solution, the GA will find the nearest solution providing a smooth data set that is needed for the ANN training. Then, with the previous data set, the ANN was trained to output the set of angles for each input voltage situation.

B. Solar Cell Modeling

A suitable model was derived to simulate the PV module behavior that reflects the experimental curves of the solar panel with relative accuracy. The single-diode model was adopted as shown in Fig. 2 to simulate the PV module under different

TABLE I
ELEVEN-LEVEL CHB SAMPLE DATA SET FOR ANN TRAINING

Input voltage (V)	*Switching angles (°)*
[25 25 25 25 25]	[0.4 9.8 19.4 26.0 41.6]
[25 25 29 35 39]	[5.0 16.5 19.8 35.7 58.4]
...	...
[33 35 35 35 39]	[7.2 28.9 41.4 52.1 73.5]
[35 35 37 37 39]	[17.7 31.4 48.8 57.5 67.7]
[36 38 40 40 40]	[21.5 37.5 51.7 58.8 70.8]

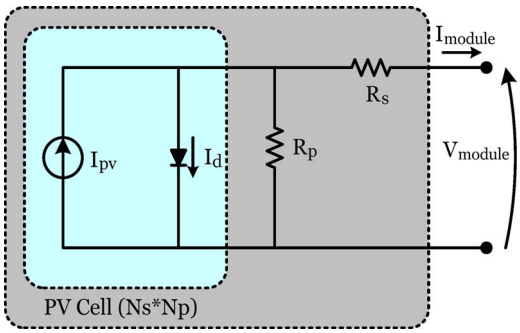

Fig. 2. PV cell single-diode model representation.

irradiance and temperature levels. A number of approaches and models can be found in the literature to analyze the behavior of PVs that can grow in complexity if even better accuracy is needed [18]–[21]. The suitable model then becomes application dependent.

The PV cell model used in this work is a more intuitive model based on the single-diode cell (Fig. 2) and derived in [21]. The inputs used are those obtained directly from the PV module data sheet parameters, which are readily available from a panel's manufacturer. This model greatly simplifies the modeling task once the iterations and nonlinear equations are solved. Equation (2) is the basic formula, and the solar panel's data sheet provides the parameters to solve for the unknowns

$$I = I_{\rm PV} - I_0 \left[e^{\left(\frac{V+R_s I}{V_t a}\right)} - 1 \right] - \frac{V + R_s I}{R_p} \qquad (2)$$

where

I PV module output current;
V PV module output voltage;
$I_{\rm PV}$ PV current;
I_0 saturation current;
V_t thermal voltage;
R_s equivalent series resistance;
R_p equivalent parallel resistance;
a diode ideality constant.

The solar panel to be connected to the H-bridge inverter is a 195-W Sanyo HIT. Its specifications and simulated parameters for use with (2) are shown in Tables II and III, respectively.

Fig. 3 compares the model obtained from the PV data sheet with the manufacturer's experimental curve to show the performance of the model. The power-versus-voltage curve also matches the manufacturer's experimental data at the same level of accuracy as Fig. 3.

TABLE II
SIMULATED PARAMETERS FOR (2)

Parameter	*Value*
I_{pv}	3.794 A
I_0	9.68×10^{-10} A
V_t	2.466 V
a	1.25
R_s	1.0973 Ω
R_p	1060.0 Ω

TABLE III
SANYO HIT PV MODULE ELECTRICAL SPECIFICATIONS

Model	*HIP-195BA19*
Rated Power (Pmax)	195 W
Max. Power Voltage (Vpm)	55.3 V
Max. Power Current (Ipm)	3.53 A
Open Circuit Voltage (Voc)	68.1 V
Short Circuit Current (Isc)	3.79 A
Temperature Coefficient (Voc)	-0.17 V/°C
Temperature Coefficient (Isc)	0.87 mA/°C

III. ANNs

ANNs have found a number of applications in engineering such as pattern recognition, control, and classification, among others [22]–[25]. One of the main factors for choosing this technique is its generalization ability in nonlinear problems that are complex in nature and/or calculation intensive [26].

The basic network chosen is shown in Fig. 4. It is a multilayer network with one input stage, two hidden layers, and one output layer. The basic computational model of a biological neuron is highlighted in Fig. 4, showing its interconnections in the network. Its inputs are the five voltage magnitudes measured at the terminals, and its output is the input for all the neurons in the next layer.

Each neuron a_j computes a weighted sum of its n inputs V_k, $k = 1, 2, \ldots, n$, and generates an output as shown in

$$a_j = tgsig\left(\sum_{k=1}^{n} w_k V_k + bias\right). \qquad (3)$$

The output is given by the tangent sigmoid of the resultant weighted sum that usually has a bias associated to it that can be considered as an additional input. In (3), w_k represents the synapse weight associated to each one of the n inputs.

A. Learning From Data

Given the data set of inputs and desired outputs, a network needs to be found that not only can generate the desired output

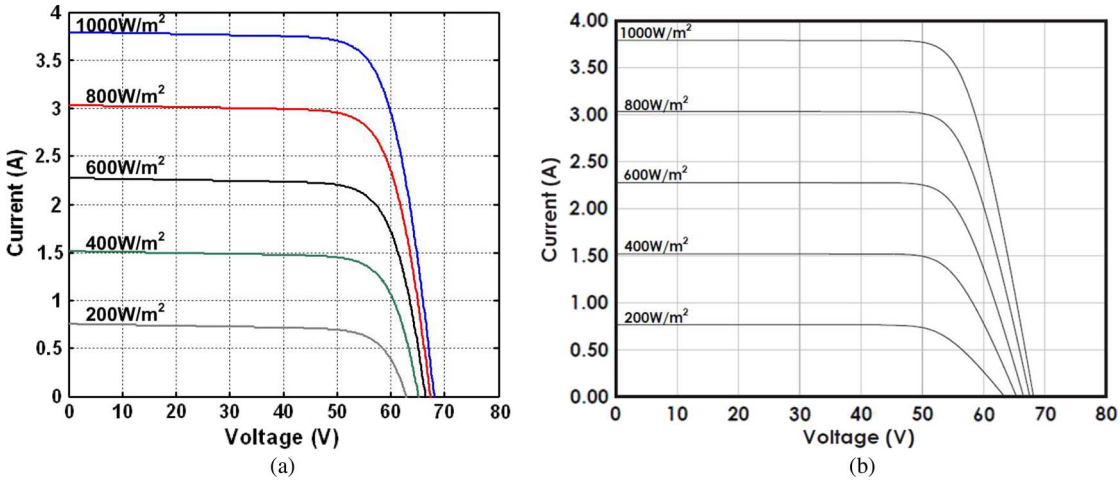

Fig. 3. (a) Simulated and (b) experimental I–V curves for the Sanyo HIT 195-W PV module.

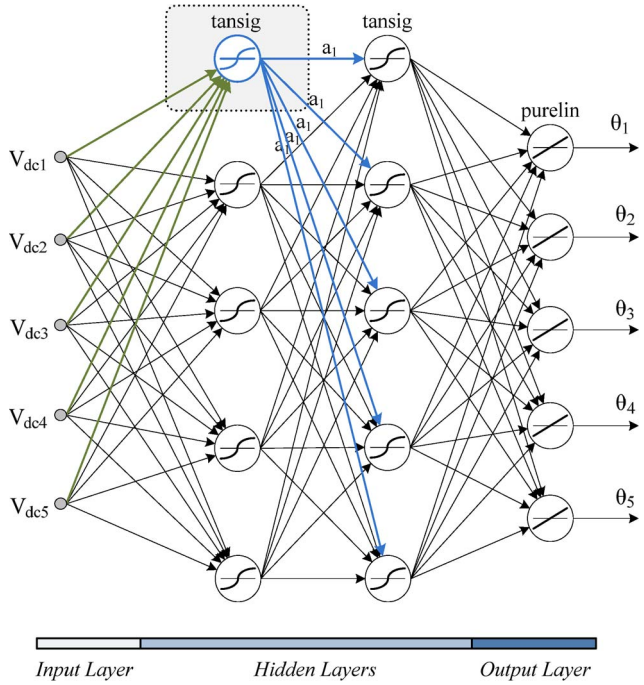

Fig. 4. Multilayer feedforward perceptron neural network model.

for the trained data but also must have the ability to generalize for points inside the hypercube space determined by the data.

Learning for the computational neuron is basically updating the network weights according to the data presented so as to efficiently represent and generalize the data set.

Performance is measured by calculating the mean-square error (mse) as shown in

$$e = \frac{1}{p}\sum_{i=1}^{p}\left\|y^{(i)} - d^{(i)}\right\|^2 \tag{4}$$

where

p number of training data entries;
y ANN output vector-current ANN output;
d desired output vector-switching angles.

The ANN backpropagation training algorithm uses the error obtained in (4) to update the weights so as to minimize the error. For a set of input voltages, a well-trained ANN would output switching angles that are very close to the desired values, giving an error near zero in (4). The desired switching angles are those that minimize the harmonic components while keeping the fundamental voltage.

B. SHE Data Set

The number of possible combinations that generates the data set for ANN training is exponentially increased by the number of H-bridges in the topology. For a two-full-bridge case (five levels) considering a data set of four voltage levels for training, for example, [45 V, 50 V, 55 V, 60 V] would generate a table of 4^2 rows. In a five-H-bridge converter with ten points equally spaced between 50 and 60 V, it would generate 10^5 different combinations. In an effort to reduce the size of the data set, the problem is faced as a combination problem instead of a permutation. In this way, the data set can be greatly reduced by considering, for example, the voltage vector $v_1 = [45\ 45\ 50\ 55\ 50]$ as being the same input as $v_2 = [45\ 50\ 45\ 50\ 55]$.

C. ANN Training

The original data set was divided into three subsets: training, validation, and test. The first subset is used to train the ANN using the scaled conjugate gradient algorithm. This algorithm is a gradient descent method that updates the network weights so as to minimize the mse cost function. A validation subset is used to stop the training to avoid generalization. If the validation error starts to increase, it means that the network might be overfitting data. A third subset is used to verify that the data are not poorly divided. When this error gets a low value in a different iteration than the validation and training subsets, it might be an indication of poor data division. The proportions adopted in this work were 55% for training, 30% for validation, and 15% for test.

A total of 32 different networks were trained 50 times each, and their performance values are shown in Fig. 5. A second layer with more than 50 neurons causes the validation error to be greater than the training error, indicating that overfitting

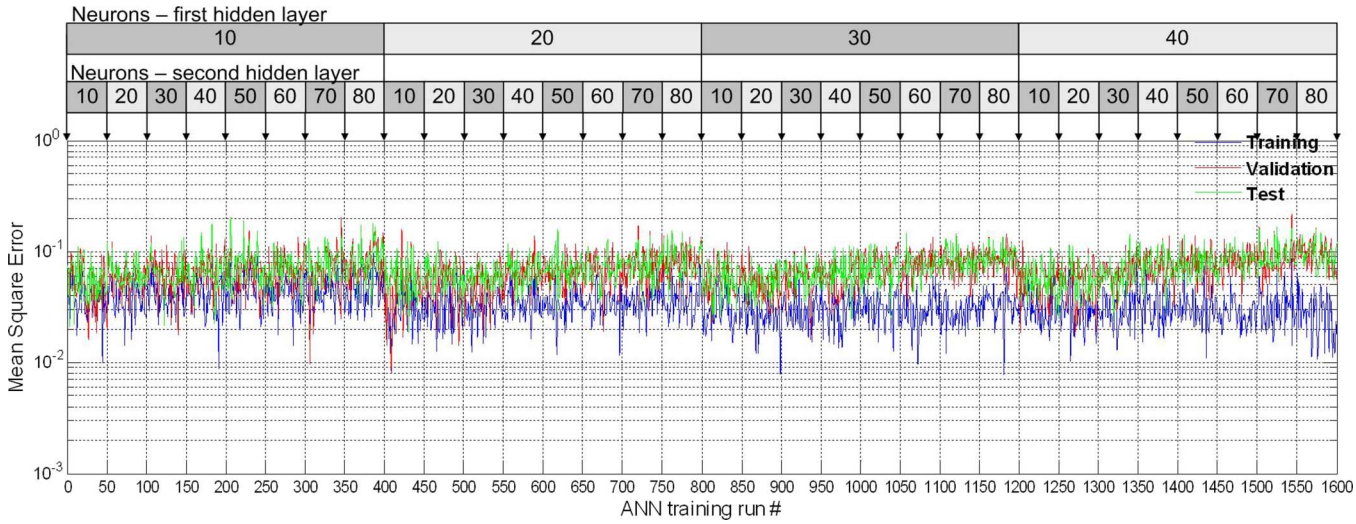

Fig. 5. ANN performance results for different numbers of hidden layer neurons.

might be occurring. In addition, with fewer than 20 neurons in each layer, an equivalent performance can be obtained as with 30 or more neurons in each layer. A look at the average values indicates that an architecture with 20 neurons in the first layer and 10 neurons on the second layer is suitable for this application.

The ANN that was implemented and is shown in Figs. 1 and 4 is a feedforward multilayer perceptron with one hidden layer of 20 neurons and second hidden layer of 10 neurons that are interconnected through weighting functions. This configuration was chosen over other designs, such as single- and multiple-hidden-layer ANNs. The two-hidden-layer performance is shown in Fig. 5. Due to better performance, training time, memorization, and learning ability, the two-hidden-layer ANN was chosen.

IV. Experimental Results

The implemented system is shown in Fig. 6. Each full bridge in the cascade topology has a 1-mF dc electrolytic capacitor and four 200-V/40-A MOSFETs. An OPAL-RT Lab is a hardware-in-the-loop system that allows real-time control of the system. The control topology used in this experiment uses two computers: One is the main station where Simulink is installed and the control is implemented (master station); the second computer has the analog and digital I/Os to control the inverter and acquire signals (slave station). Compared to DSPs, this system has a shorter implementation and debugging time as a result of a user-friendly interface; however, this comes at the cost of a sample time that can range from 50 to 150 μs in this particular setup. This can reflect in up to 1° divergence from the software-calculated ANN angles in some cases.

Fig. 7 shows a 100-ms window of the 11-level cascade inverter running with solar panels as its input source. During this time period, a load step was applied to the inverter output, causing the panels' voltage to drop. This voltage drop can be observed in channel 3 (purple) that is an indoor solar panel. This figure illustrates a resistive step change applied at the output that causes a slow voltage drop also helped by the energy stored in the capacitance. In the second channel (cyan),

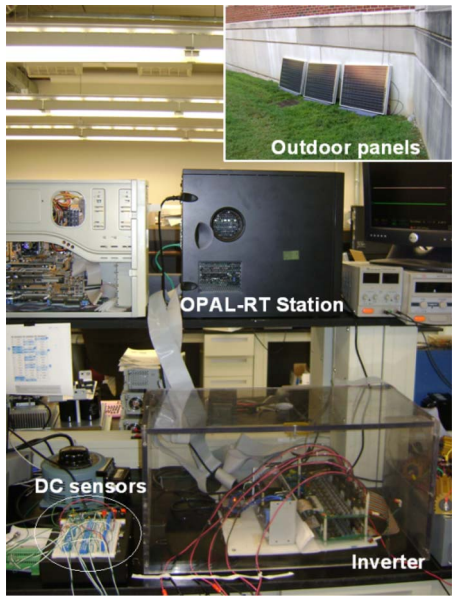

Fig. 6. Experimental ML setup and PV panels' installation.

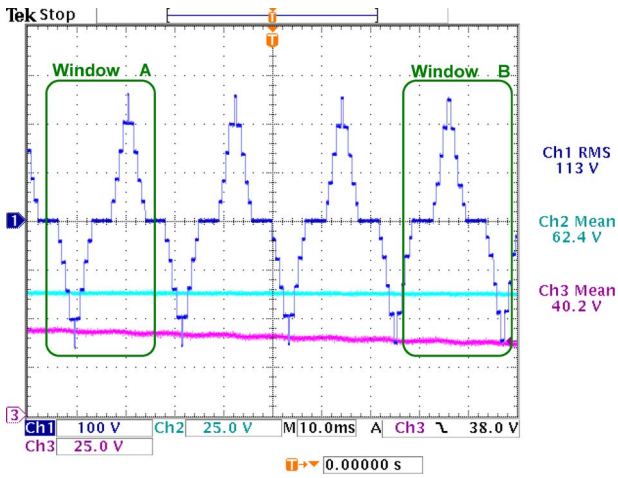

Fig. 7. (Blue) Real-time change in output voltage angle generation by the ANN after (purple) voltage variation of one of its dc inputs.

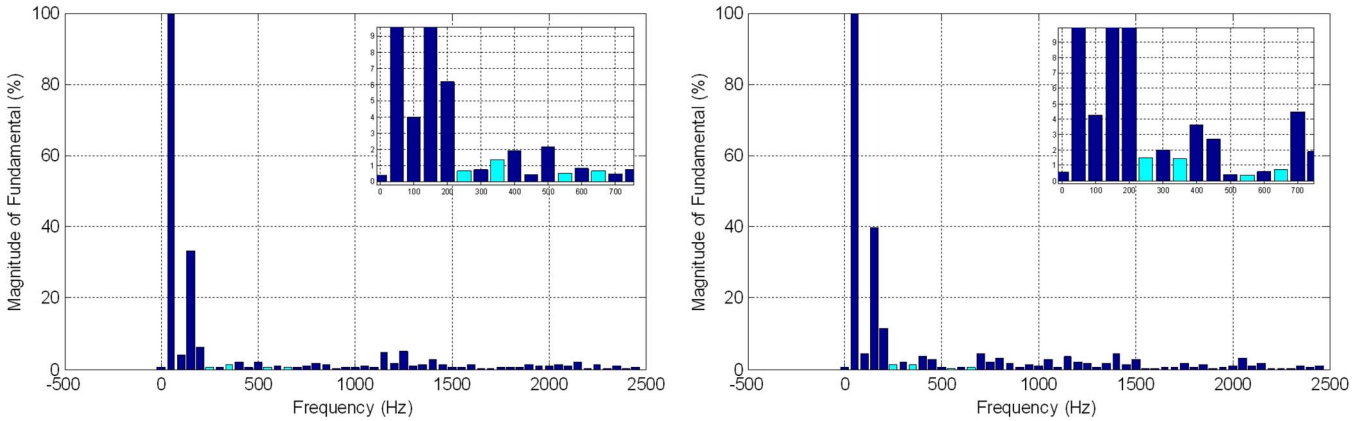

Fig. 8. Frequency spectrum content for windows A and B, respectively, as a percentage of the 120-V fundamental.

which is sensing an outdoor solar panel, the effect of the load step was not heavy enough to cause significant voltage drop mainly because those panels, at the time of the experiment, were subjected to a larger level of irradiance as a consequence of its orientation and time of the day.

In the same figure in the third channel (purple), a voltage drop can be seen as a result of the load change. From an initial value of 43.3 V dc, the solar panel output voltage drops smoothly, also helped by the 1000-μF electrolytic capacitor in the ML converter, to a value of around 36.2 V dc at the end of the acquired 100-ms window. As the voltage level decreases, a new set of switching angles is calculated by the ANN to be updated at the next fundamental cycle (50 or 60 Hz). The two windows shown in this figure (A and B) were used to do a frequency spectrum analysis of the waveform. The change in the angles can be noticed when the two windows are compared (A and B).

The spectrum content of both windows (A and B) is shown in Fig. 8. The presence of dc and even harmonic components happens as a result of the varying voltage. It is considered in this work that such large voltage variation rate is not likely to happen, and if it occurs, it is a transitory state where the angles are updated at the cost of even and/or dc transient components. The total harmonic distortion is greater than the expected range of 7%–14% as a consequence of those components added up by the voltage transient. Harmonics are not completely eliminated in this approach but instead minimized. The target harmonics were kept at less than 1.5% of the fundamental as it can be seen in both windows. A zoomed window is shown in the upper right corner with the 5th, 7th, 11th, and 13th components (cyan). The expected target harmonic levels obtained by the experiment are higher due to a considerably high hardware sample time during execution. The second highest component in the plots is the third harmonic, which is not considered a harmful component for three-phase applications.

Fig. 9 shows the output voltage for the same inverter operating with nine levels under a resistive 100-Ω load with PV panels. The harmonic levels are indicated in the picture as a percentage of the fundamental value with the fifth harmonic at 1.5% of the fundamental voltage ($V_{\text{fund}} = 117.8$ V). Fig. 10 shows both output voltage and frequency spectra on the same plot with the harmonic components of interest indicated in the

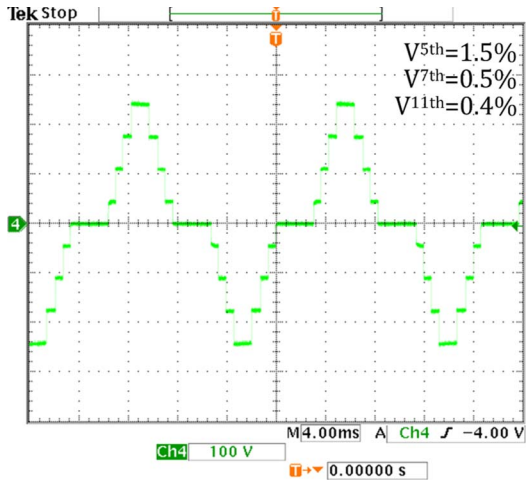

Fig. 9. Experimental output voltage and harmonic performance for a 120-V line-to-neutral ML inverter.

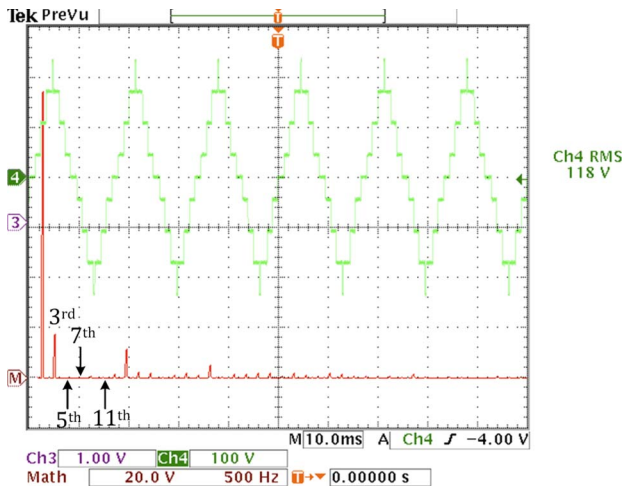

Fig. 10. Experimental output voltage and frequency spectra with the target harmonics indicated.

picture. The target harmonics in this case are under 1% of the fundamental voltage ($V_{\text{fund}} = 118.0$ V). Both Figs. 9 and 10 were taken during a full day of operation and represent ANN angle generation for two points of operation, while Fig. 7 shows the ANN ability to update angles over the cycle.

V. Conclusion

The analytic calculation of the angles in real time for harmonic elimination is still being studied and approached by researchers through different paths. This paper has investigated ANNs as a tool to provide the angles in-cycle (50 or 60 Hz) that also can have DSP implementation but at the cost of minimization of harmonics instead of elimination. The ANN was trained with a mixed data set that has eliminated harmonics and, for those points where a solution does not exist, minimized harmonics. The real-time performance over a 100-ms window was shown to validate the proposed approach.

The output angles returned by the ANN may not provide a satisfactory result, or harmonic elimination, at some points as it generalizes; however, a fast result can be obtained, and more angles can be easily added to provide a better output waveform. Parallel networks can be used to accomplish better performance also.

Future work points in the direction of implementation and performance evaluation on a DSP platform as well as system performance over a greater number of angles. In addition, as an efficient way, to combine ANN and maximum power point tacking of solar panels will also be a topic of research.

References

[1] J. Rodriguez, J. Lai, and F. Z. Peng, "Multilevel inverters: A survey of topologies, control and applications," *IEEE Trans. Ind. Electron.*, vol. 49, no. 4, pp. 724–738, Aug. 2002.

[2] A. Pandey, B. Singh, B. N. Singh, A. Chandra, K. Al-Haddad, and D. P. Kothari, "A review of multilevel power converters," *Inst. Eng. J. (India)*, vol. 86, pp. 220–231, Mar. 2006.

[3] J. R. Wells, P. L. Chapman, and P. T. Krein, "Generalization of selective harmonic control/elimination," in *Proc. IEEE Power Electron. Spec. Conf.*, Jun. 2005, pp. 1358–1363.

[4] B. Ozpineci, L. M. Tolbert, and J. N. Chiasson, "Harmonic optimization of multilevel converters using genetic algorithms," *IEEE Power Electron. Lett.*, vol. 3, no. 3, pp. 92–95, Sep. 2005.

[5] J. N. Chiasson, L. M. Tolbert, K. J. McKenzie, and Z. Du, "A unified approach to solving the harmonic elimination equations in multilevel converters," *IEEE Trans. Power Electron.*, vol. 19, no. 2, pp. 478–490, Mar. 2004.

[6] J. N. Chiasson, L. M. Tolbert, K. J. McKenzie, and Z. Du, "Elimination of harmonics in a multilevel converter using the theory of symmetric polynomials and resultants," *IEEE Trans. Control Syst. Technol.*, vol. 13, no. 2, pp. 216–223, Mar. 2005.

[7] Z. Du, L. M. Tolbert, J. N. Chiasson, and H. Li, "Low switching frequency active harmonic elimination in multilevel converters with unequal DC voltages," in *Conf. Rec. IEEE IAS Annu. Meeting*, Oct. 2005, pp. 92–98.

[8] Z. Du, L. M. Tolbert, and J. N. Chiasson, "Active harmonic elimination for multilevel converters," *IEEE Trans. Power Electron.*, vol. 21, no. 2, pp. 459–469, Mar. 2006.

[9] D. Ahmadi and J. Wang, "Selective harmonic elimination for multilevel inverters with unbalanced DC inputs," in *Proc. IEEE Veh. Power Propulsion Conf.*, Sep. 2009, pp. 773–778.

[10] M. Dahidah and V. G. Agelidis, "Selective harmonic elimination multilevel converter control with variant DC sources," in *Proc. IEEE Conf. Ind. Electron. Appl.*, May 2009, pp. 3351–3356.

[11] M. G. H. Aghdam, S. H. Fathi, and G. B. Gharehpetian, "Elimination of harmonics in a multi-level inverter with unequal DC sources using the homotopy algorithm," in *Proc. IEEE Int. Symp. Ind. Electron.*, Jun. 2007, pp. 578–583.

[12] T. Tang, J. Han, and X. Tan, "Selective harmonic elimination for a cascade multilevel inverter," in *Proc. IEEE Int. Symp. Ind. Electron.*, Jul. 2006, pp. 977–981.

[13] J. R. Wells, B. M. Nee, and P. L. Chapman, "Selective harmonic control: A general problem formulation and selected solutions," *IEEE Trans. Power Electron.*, vol. 20, no. 6, pp. 1337–1345, Nov. 2005.

[14] M. S. A. Dahidah and V. G. Agelidis, "Selective harmonic elimination PWM control for cascaded multilevel voltage source converters: A generalized formula," *IEEE Trans. Power Electron.*, vol. 23, no. 4, pp. 1620–1630, Jul. 2008.

[15] D. W. Kang, H. C. Kim, T. J. Kim, and D. S. Hyun, "A simple method for acquiring the conducting angle in a multilevel cascaded inverter using step pulse waves," *Proc. Inst. Elect. Eng.—Elect. Power Appl.*, vol. 152, no. 1, pp. 103–111, Jan. 2005.

[16] Y. Liu, H. Hong, and A. Q. Huang, "Real-time calculation of switching angles minimizing THD for multilevel inverters with step modulation," *IEEE Trans. Ind. Electron.*, vol. 56, no. 2, pp. 285–293, Feb. 2009.

[17] F. J. T. Filho, L. M. Tolbert, Y. Cao, and B. Ozpineci, "Real time selective harmonic minimization for multilevel inverters connected to solar panels using artificial neural network angle generation," in *Proc. IEEE Energy Convers. Congr. Expo.*, Sep. 2010, pp. 594–598.

[18] U. Boke, "A simple model of photovoltaic module electric characteristics," in *Proc. Eur. Conf. Power Electron. Appl.*, Sep. 2007, pp. 1–8.

[19] O. Gil-Arias and E. I. Ortiz-Rivera, "A general purpose tool for simulating the behavior of PV solar cells, modules and arrays," in *Proc. 11th Workshop Control Model. Power Electron.*, Aug. 2008, pp. 1–5.

[20] R. Ramaprabha and B. L. Mathur, "MATLAB based modeling to study the influence of shading on series connected SPVA," in *Proc. 2nd Int. Conf. Emerging Trends Eng. Technol.*, Dec. 2009, pp. 30–34.

[21] M. G. Villalva, J. R. Gazoli, and E. R. Filho, "Comprehensive approach to modeling and simulation of photovoltaic arrays," *IEEE Trans. Power Electron.*, vol. 24, no. 5, pp. 1198–1208, May 2009.

[22] J. J. Hopfield, "Artificial neural networks," *IEEE Circuits Devices Mag.*, vol. 4, no. 5, pp. 3–10, Sep. 1988.

[23] R. Aggarwal and Y. Song, "Artificial neural networks in power systems II: Types of artificial neural networks," *Power Eng. J.*, vol. 12, no. 1, pp. 41–47, Feb. 1998.

[24] R. Aggarwal and Y. Song, "Artificial neural networks in power systems I: General introduction to neural computing," *Power Eng. J.*, vol. 11, no. 3, pp. 129–134, Jun. 1997.

[25] M. J. Willis, C. Di Massimo, G. A. Montague, M. T. Tham, and A. J. Morris, "Artificial neural networks in process engineering," *Proc. Inst. Elect. Eng.—Control Theory Appl.*, vol. 138, no. 3, pp. 256–266, May 1991.

[26] A. K. Jain, J. Mao, and K. M. Mohiuddin, "Artificial neural networks: A tutorial," *Computer*, vol. 29, no. 3, pp. 31–44, Mar 1996.

Faete Filho (S'08) received the B.S. and M.S. degrees in electrical engineering from the Federal University of Mato Grosso do Sul, Campo Grande, Brazil, in 2004 and 2006, respectively. He is currently working toward the Ph.D. degree at The University of Tennessee, Knoxville (UTK).

He was an Associate Researcher with the Batlab Research Laboratory, Brazil, in 2007. His team was awarded outstanding educational impact and first place in the 2005 and 2007 IEEE Future Energy Challenge competition, respectively. He is currently a Student Leader designing and building a house for the UTK team for the 2011 Solar Decathlon competition. He is an active Representative in the student graduate senate and an occasional Reviewer for IEEE Transactions and conferences. His current areas of interest include multilevel inverters, power converters for distributed energy resources, and artificial intelligence techniques and applications to power electronics.

Leon M. Tolbert (S'88–M'91–SM'98) received the Bachelor's, M.S., and Ph.D. degrees in electrical engineering from the Georgia Institute of Technology, Atlanta, in 1989, 1991, and 1999, respectively.

He was with the Engineering Division, Oak Ridge National Laboratory (ORNL), Oak Ridge, TN, from 1991 to 1999. He was appointed as an Assistant Professor in the Department of Electrical and Computer Engineering, The University of Tennessee, Knoxville (UTK), in 1999. He was a Visiting Professor at Zhejiang University, Hangzhou, China, in 2010. He is currently the Min Kao Professor in the Department of Electrical Engineering and Computer Science, UTK. He is also a Research Engineer with the Power Electronics and Electric Machinery Research Center, ORNL, Knoxville.

Dr. Tolbert is a Registered Professional Engineer in the State of Tennessee. He was the recipient of a 2001 National Science Foundation CAREER Award, the 2001 IEEE Industry Applications Society Outstanding Young Member Award, and three prize paper awards from the IEEE Industry Applications Society and the IEEE Power Electronics Society. He was the Chairman of the Educational Activities Committee of the IEEE Power Electronics Society and an Associate Editor of the IEEE POWER ELECTRONICS LETTERS from 2003 to 2006. He has been an Associate Editor of the IEEE TRANSACTIONS ON POWER ELECTRONICS since 2007. He was elected to serve as a Member-at-Large of the IEEE Power Electronics Society Advisory Committee for 2010–2012.

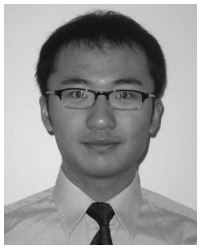

Yue Cao (S'08) received the B.S. degree in electrical engineering (with honors) and double major in mathematics from The University of Tennessee, Knoxville (UTK), in 2011. He is currently working toward the M.S. degree in power and energy area of electrical engineering at the University of Illinois at Urbana-Champaign, Champaign.

He was an Undergraduate Research Assistant with the Power and Energy Laboratory, UTK, from 2008 to 2011. He interned at Memphis Light, Gas and Water as a Power Engineer in summer 2009. He was an Intern Research Assistant at Oak Ridge National Laboratory, Oak Ridge, TN, in summer 2010.

Mr. Cao is a member of the IEEE Power and Energy Society, the IEEE Power Electronics Society, Theta Tau Professional Engineering Fraternity, and the *UTK Undergraduate Research Journal* Editorial Board. He also served as the Webmaster for the 2009, 2010, and 2012 IEEE Energy Conversion Congress and Exposition. He has received awards, including the UTK Chancellor Citation Award, UTK undergraduate summer research fellowship, electrical engineering outstanding student of the year, and U.S. Math Olympiad national finalist.

Burak Ozpineci (S'92–M'02–SM'05) received the B.S. degree in electrical engineering from Middle East Technical University, Ankara, Turkey, in 1994, and the M.S. and Ph.D. degrees in electrical engineering from The University of Tennessee, Knoxville (UTK), in 1998 and 2002, respectively.

He joined the Postmasters Program of the Power Electronics and Electric Machinery Research Center, Oak Ridge National Laboratory (ORNL), Knoxville, in 2001, and became a full-time Research and Development Staff Member in 2002 and the Group Leader of the Power and Energy Systems Group in 2008. He is currently the Group Leader for the Power Electronics and Electric Machinery Group, and he also has a Joint Faculty Associate Professor position with The University of Tennessee. His research interests include system-level impact of SiC power devices, multilevel inverters, power converters for distributed energy resources and hybrid electric vehicles, and intelligent control applications for power converters.

Dr. Ozpineci is the Chair of the Rectifiers and Inverters Technical Committee of the IEEE Power Electronics Society and was the Transactions Review Chairman of the Industrial Power Converter Committee of the IEEE Industry Applications Society. He was the recipient of the 2001 IEEE International Conference on Systems, Man, and Cybernetics Best Student Paper Award, the 2005 UT-Battelle (ORNL) Early Career Award for Engineering Accomplishment, and the 2006 IEEE Industry Applications Society Outstanding Young Member Award.